HIGH REPETITION RATE COMPACT MARX GENERATOR

M. M. Kekez*
High-Energy Frequency Tesla Inc. (HEFTI)
1200 Montreal Road, NRC Site, Bldg. M-51, Ottawa, Ontario, Canada, K1A 0R6

Abstract

The charging of a compact generator has been accomplished with the network suggested by O'Loughin et al. [1]. The research for the suitable ceramic magnet cores was carried out for square-shaped output pulses lasting 1000 ns in duration.

The generator is used to broaden our knowledge in the radio frequency (RF) generation and supplement the data obtained at low RF range at 1 GW power levels reported in reference [2].

I. INTRODUCTION

In the classical electromagnetic pulse (EMP), the Marx generator discharged into a resistive load produces a pulse with a short rise-time and a long exponential fall. New types of loads have been recently developed where the voltage waveform is modulated and the current trace is a semi-smooth function of time. See Figure 1. These modulations cause the radio frequencies emissions here named the Non Nuclear (NN)-EMP. The spectrum of the NN-EMP system is broad and ranges from tens of MHz to a few GHz. The NN-EMP systems can be tuned to operate mainly at a single frequency in the RF domain.

The NN-EMP emissions are found to be reproducible and predictable. At a single frequency the energy of the RF pulse, E scales as $E \sim V^2$, where V is the charging voltage per stage of the Marx generator.

II. CHARGING OF THE MARX GENERATOR

The charging of a compact Marx generator at high repetition rates has been accomplished by replacing the conventional resistive charging network by the inductor configuration as suggested by O'Loughin et al. [1]. Using their method, the two parallel inductors in each stage of the network ladder were wound on a single ceramic magnetic core.

The research for suitable ceramic magnet cores was carried out by using the pulsed forming network (PFN). For this purpose, a separate two-stage Marx generator was assembled. Each stage had 10 TDK capacitors charged to 7.5 kV. Each capacitor had 1.7 nF. There were nine inductors in the PFN, each having L of 2.1 μH.

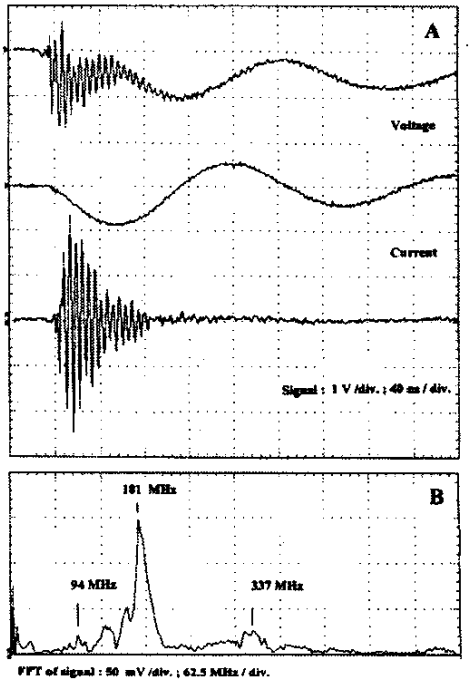

Figure 1. Voltage, current, and radiations (signal) with its FFT of the basic NN-EMP system.

The theoretical value of the pulse width of PFN:

$$T = 2\sqrt{(9L)(10C)} = 18.97\sqrt{(2.1\times10^{-6})(1.7\times10^{-9})} = 1129\,\text{ns}$$

The characteristic impedance is

$$Z_0 = \sqrt{L/C} = \sqrt{(2.1\times10^{-6})/(1.7\times10^{-9})} = 35\ \Omega$$

The experimental value used was 37.5 Ω, because the output voltage (at the second stage) was terminated with a 75 Ω resistor.

Cores of different sizes were investigated. Some of the findings are summarized in Table 1 and in Figure 2, Frame A.

Table 1.

	I.D. (cm)	O.D. (cm)	Height (cm)	Number of windings in single coil	Inductance of single coil, L (μH)	Total L during charging/stage (μH)
small size core	3.2	4.9	1.9	8	226	6.5
medium size core	6.0	10.0	1.6	21	890	59
large size core	10.0	19.0	2.54	35	4950	375

* email: mkekez@magma.ca

0-7803-7915-2/03/$17.00 ©2003IEEE.

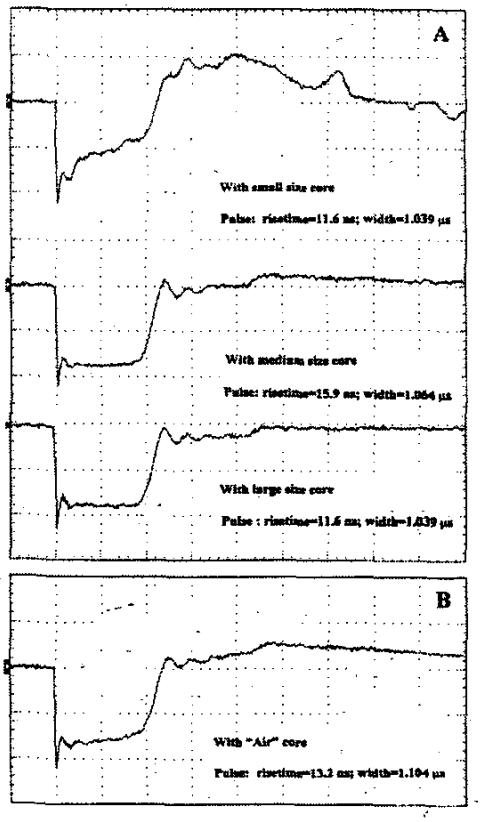

Figure 2. Output voltage as function of the inductive charging arrangement. The time scale is 500ns/div

Table 2.

	O.D. (cm)	Length (cm)	Number of windings in coil	Inductance of coil, L (µH)
air core coil	4.4	5.9	59	107

An air core coil was also used for the purpose of comparison. Its characteristics are given in Table 2 and Figure 2, Frame B.

The values of the inductances given in Tables 1 and 2 are the small-signal data obtained using a conventional RLC instrument. The result given in Frame B should be comparable to that of the Frame A, top trace; however, this is not the case. The trace at the top in the Frame A has smaller L/R time constant in comparison to the trace in Frame B. It appears that the magnetic permeability of the ceramic magnetic core decreased as the current flowing in the coil is increased. The determining factor is the power density levels to be transferred by the core. The present method uses conventional transformer action, i.e. between two inductors placed on the same core. For effective energy transfer from one inductor to another inductor, the core must be of a sufficiently large size. [3]

The large core produced a waveform identical in shape to that obtained with a 1 MΩ charging resistor in each arm. The medium size core was adopted for the current

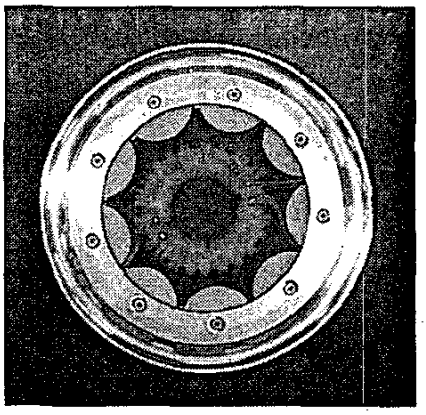

Figure 3. Photograph of the single stage with the charging coil placed in the centre.

system and placed in the centre of each stage of the Marx generator. See Figure 3.

III. THE SPARK GAP ARRANGEMENT

The spark gap electrode assembly was organized at the outer rim of the plate that holds nine capacitors. This way, a circular rail-gap switch is constructed by virtue of the distributed low-inductance "rail" geometry. It was observed that multi-channeling is achieved over the entire circumference (85 cm) of the plate. The (breakdown) switching is carried out by a weak filamentary spark channel superimposed on a weak diffuse glow background. The separation between two stages of 0.635 cm (¼") is provided by a Plexiglas ring. The grove in the plate together with the Plexiglas ring ensures that there is no current leakage during the charging cycle. The eight-stage Marx generator is achieved by putting one stage on top of another stage. The first stage also has a sharp knife-edge trigger electrode to activate the system.

The Marx generator is enclosed so that the system forms a coaxial design with the low internal impedance. Nine capacitors per module were used for a total of 72 capacitors. The capacitance per stage is 18 nF. The charging voltage varies from 12 to 32 kV per stage. The output voltage rises from 96 to 256 kV (into a high impedance load). The rise time is less than 1 ns (into a resistive load). The energy stored in the capacitors varies from 10 to 75 J. A repetition rate of 10 pulses per second (pps) was achieved with the available dc power supply. Using a two-stage system, the repetition rate reached 50 pps, when the run was done in the burst mode.

IV. EXPERIMENTAL RESULTS

The phenomena of RF generation was also confirmed with the current Marx generator. A 10GHz D-dot probe (made by Prodyne Inc.) was placed at the distance of 168 cm. If the value of the NN-EMP radiation signal is V_0 and f is the frequency, the electrical field E_0 is calculated by Equation 1.

$$E_0\ (\text{V/m}) = \frac{1.798 V_0\ (\text{mV})}{f\ (\text{GHz})} \qquad (1)$$

For multifrequency emission, it is necessary to analyse (filter out) each frequency component and evaluate the electric field, spatially and temporally, to obtain the power density, $P = E_0^2/(2*120\pi)$. To map the radiation-pattern and compute the total power, it is necessary to integrate the power density value over the solid angle of 4π. Because the variation of the field intensity from shot to shot are relatively small, only a few sensors and oscilloscopes are required.

Figures 4 and 5 give examples of the emission at low end of RF range.

In the high RF range, the discontinuities in the energy/power transfer from the generator to the NN-EMP device are manifested as the frequency line in the Fast Fourier Transform (FFT). The wealth of lines in FFT could be a sign that the system is not well matched. In addition, the lines may also appear because the generator has a high throughput time.

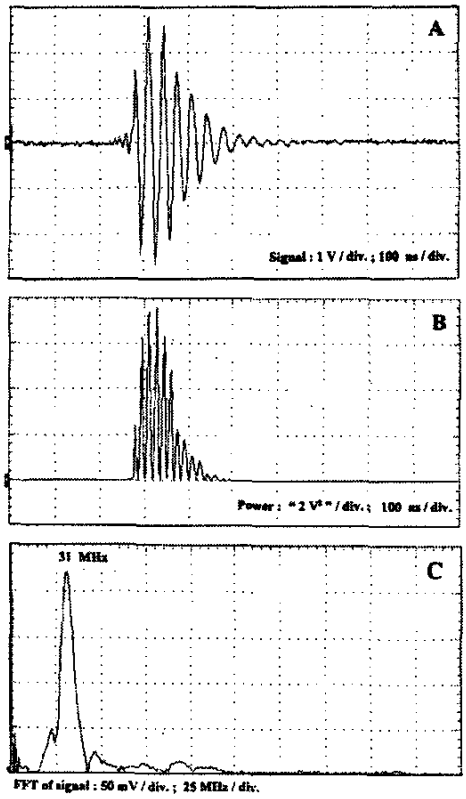

Figure 4. *RF emission at frequency of 31 MHz.* The average amplitude of RF signal (Frame A) is 2.5 V. For f=31 MHz, (Frame C), E_0 = average value of electric field = 145 kV/m and P = 2.79 kW/cm^2. For quasi cylindrical pattern of radiation, the RF power is 102 MW. For pulse width of 70 ns, the RF energy is 7.14 J. The trace power (Frame B) means multiplying the signal by itself. The generator was charged at 25 kV/stage and had stored 45 J.

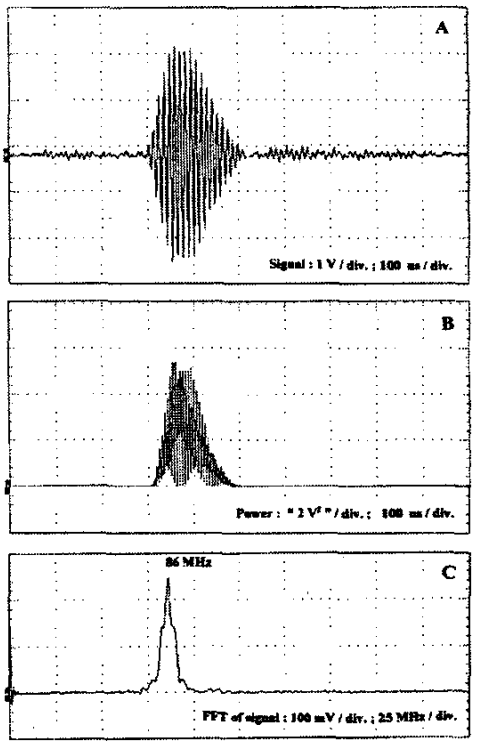

Figure 5. *RF emission at frequency of 86 MHz.* The average amplitude of RF signal (Frame A) is 2.24 V. For f=86 MHz, (Frame C), E_0 =46.83 kV/m, P=0.29 kW/cm^2. For quasi cylindrical pattern of radiation, the RF power is 10.7 MW. For pulse width of 80 ns, the RF energy is 0.85 J. Other conditions are as in Figure 4.

In Figures 6 through 8, the effects of the insulating material are shown. At the two frequencies, 249 and 146 MHz, the RF emissions are indicated in Figure 6. Note that the ratio of 249/146 is equal to $(\varepsilon_r)^{1/2}$, where ε_r is the relative dielectric constant of the material (Plexiglas) used in construction of the NN-EMP device. The higher frequency emission, 249 MHz, originated in the dielectric material where air is the main constituent.

By decreasing the amount of the insulating (plastic) material in the NN-EMP system, only the higher frequencies are recorded. The result is shown in Figure 7. Similarly, the system can be tuned to lower frequencies, and the result is shown in Figure 8.

V. CONCLUSION

The system works well and the RF results are reproducible. A repetition rate of 10 pps was achieved with the available dc power supply. Using a two-stage system, the repetition rate reached 50 pps, when the run was done in the burst mode. The system can be used for the following applications:

- RF threat assessment
- Mitigation of RF attacks and for protection of electronic infrastructure in the country
- Further development of explosively driven MCG's

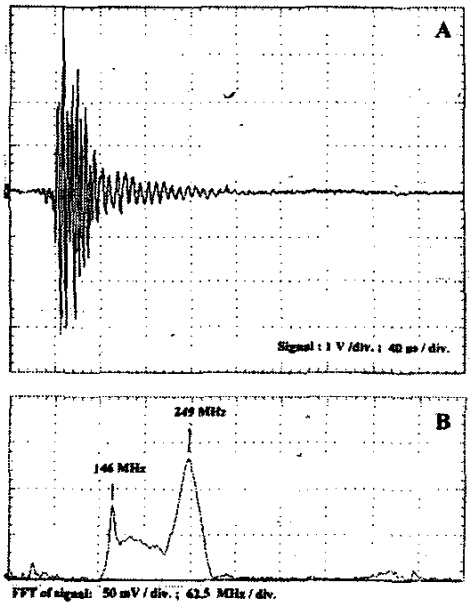

Figure 6. RF emission at two frequencies. The generator was charged at 25 kV/stage and had stored 45 J.

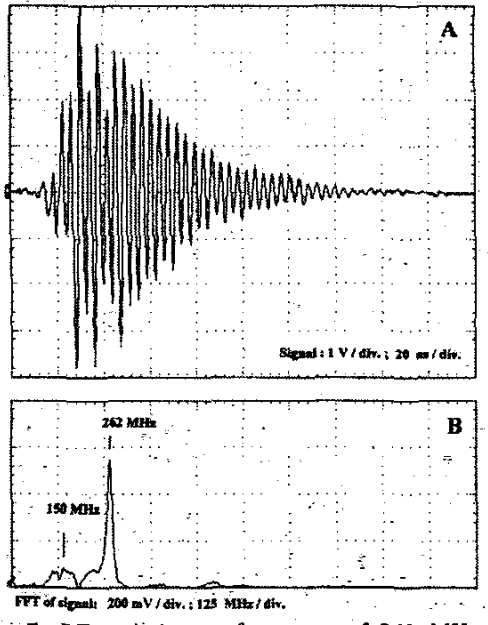

Figure 7. *RF emission at frequency of 262 MHz.* The average amplitude of RF signal (Frame A) is 2.5 V. For f = 262 MHz, (Frame C), E_0 = 17.2 kV/m, P = 39 W/cm^2. For quasi cylindrical pattern of radiation, the RF power is 1.44 MW. For pulse width of 40 ns, the RF energy is 57 mJ. Other conditions are as in Figure 4.

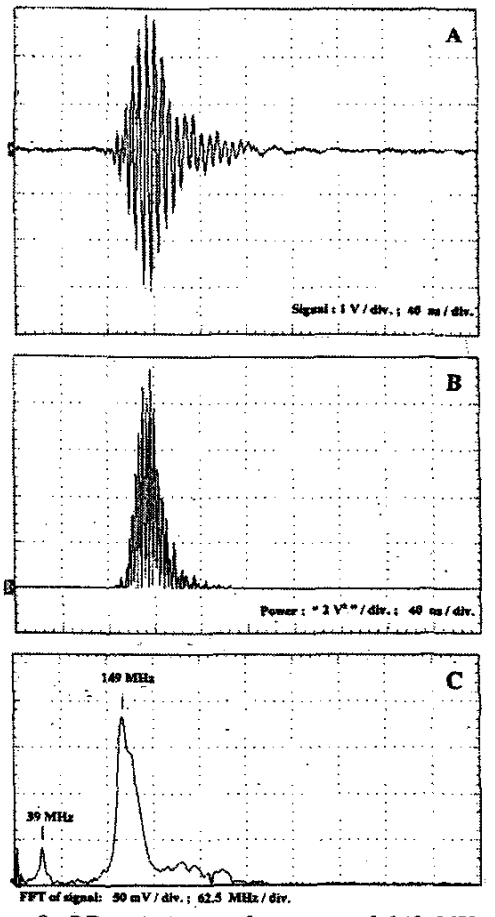

Figure 8. *RF emission at frequency of 149 MHz.* The average amplitude of RF signal (Frame A) is 2.65 V. For f = 149 MHz (Frame C), E_0 = 31.8 kV/m, P =136 W/cm^2. For quasi cylindrical pattern of radiation, the RF power is 5 MW. For pulse width of 40 ns, the RF energy is 100 mJ. Other conditions are as in Figure 4.

VI. REFERENCES

[1] J.P. O'Loughin, J.M. Lehr, and D.L. Loree, "High Repetition Rate Charging a Marx Type Generator" in Abstracts of PPPS-2001, 2001, pp. 258.

[2] M.M. Kekez, "A compact square waveform 15 kJ generator: 15 ns risetime, 7.5 Ω load impedance and 100-500 ns pulse width" in Proc. PPPS-2001, 2001, pp. 1027-1030.

[3] N.G. Glasoe and J.V. Lebacqz, Pulse Transformer. NY: McGraw-Hill, 1948.